

Structure of Human Apolipoprotein A-IV: A Distinct Domain Architecture among Exchangeable Apolipoproteins with Potential Functional Implications[†]

Kevin Pearson,[‡] Hiroyuki Saito,[§] Stephen C. Woods,^{||} Sissel Lund-Katz,[§] Patrick Tso,[‡] Michael C. Phillips,[§] and W. Sean Davidson^{*:‡}

Department of Pathology and Laboratory Medicine, University of Cincinnati, Cincinnati, Ohio 45267, Children's Hospital of Philadelphia, University of Pennsylvania School of Medicine, Philadelphia, Pennsylvania 19104-4318, and Department of Psychiatry, University of Cincinnati, Cincinnati, Ohio 45267

Received May 19, 2004; Revised Manuscript Received June 24, 2004

ABSTRACT: Apolipoprotein A-IV (apoA-IV) is an exchangeable apolipoprotein that shares many functional similarities with related apolipoproteins such as apoE and apoA-I but has also been implicated as a circulating satiety factor. However, despite the fact that it contains many predicted amphipathic α -helical domains, relatively little is known about its tertiary structure. We hypothesized that apoA-IV exhibits a characteristic functional domain organization that has been proposed to define apoE and apoA-I. To test this, we created truncation mutants in a bacterial system that deleted amino acids from either the N- or C-terminal ends of human apoA-IV. We found that apoA-IV was less stable than apoA-I but was more highly organized in terms of its cooperativity of unfolding. Deletion of the extreme N and C termini of apoA-IV did not significantly affect the cooperativity of unfolding, but deletions past amino acid 333 on the C terminus or amino acid 61 on the N terminus had major destabilizing effects. Functionally, apoA-IV was less efficient than apoA-I at clearing multilamellar phospholipid liposomes and promoting ATP-binding cassette transporter A1-mediated cholesterol efflux. However, deletion of a C-terminal region of apoA-IV, which is devoid of predicted amphipathic α helices (amino acids 333–376) stimulated both of these activities dramatically. We conclude that the amphipathic α helices in apoA-IV form a single, large domain that may be similar to the N-terminal helical bundle domains of apoA-I and apoE but that apoA-IV lacks the C-terminal lipid-binding and cholesterol efflux-promoting domain present in these apolipoproteins. In fact, the C terminus of apoA-IV appears to reduce the ability of apoA-IV to interact with lipids and promote cholesterol efflux. This indicates that, although apoA-IV may have evolved from gene duplication events of ancestral apolipoproteins and shares the basic amphipathic helical building blocks, the overall localization of functional domains within the sequence is quite different from apoA-I and apoE.

Apolipoprotein A-IV (apoA-IV)¹ is a 46-kDa protein discovered in 1974 in rat plasma high-density lipoprotein (HDL) (1). In humans, it is synthesized by the small intestine and secreted into the mesenteric lymphatics associated with chylomicrons. Under conditions of high lipid absorption, apoA-IV secretion by the gut is up-regulated and can account for up to 3% of the total gut-secreted protein (2, 3). Upon chylomicron lipolysis in the general circulation, apoA-IV

rapidly dissociates from remnant particles, primarily residing in HDL and as lipid-poor protein (2, 4). Despite this responsiveness to lipid intake, an unambiguous function for apoA-IV has not yet been widely recognized. It has been proposed to play many functions in vivo, including food intake regulation (5), gastrointestinal motility (6), structural constituent of lipoproteins (7), and protection against lipid oxidation and atherosclerosis (8), and can also mimic many of the roles of apoA-I, including cholesterol efflux and activation of lecithin:cholesterol acyl transferase (9, 10).

ApoA-IV shares several general features with other exchangeable apolipoproteins, especially apoA-I and apoE. The primary sequences of all three proteins are dominated by multiple 22 amino acid repeats, which are predicted to form amphipathic α helices (11). These repeats are likely responsible for the ability of these proteins to associate with lipids. ApoA-IV contains at least 12 such repeats of which most are punctuated by proline residues (11). However, the majority of its repeats are significantly more hydrophilic than the helices within apoA-I and apoE, making it the most hydrophilic of the human exchangeable apolipoproteins. As a result, its helices have been proposed to penetrate less deeply into lipid than the helices of other apolipoproteins

[†] This work was supported by National Institutes of Health Grants HL62542 (to W.S.D.) and HL22633 (to M.C.P.).

* To whom correspondence should be addressed: Genome Research Institute, 2120 E. Galbraith Rd., Building A ML 0507, Cincinnati, OH 45237. E-mail: sean.davidson@uc.edu.

[‡] Department of Pathology and Laboratory Medicine, University of Cincinnati.

[§] University of Pennsylvania School of Medicine.

^{||} Department of Psychiatry, University of Cincinnati.

¹ Abbreviations: ABCA1, ATP-binding cassette transporter A1; ANS, 8-anilino-1-naphthalenesulfonic acid; apoA-I, apolipoprotein A-I; apoA-IV, apolipoprotein A-IV; apoE, apolipoprotein E; BSA, bovine serum albumin; BS₃, bis[sulfosuccinimidyl] suberate; CD, circular dichroism; DMEM, Dulbecco's modified Eagle medium; DMPC, dimyristoyl phosphatidylcholine; DMSO, dimethyl sulfoxide; HDL, high-density lipoprotein; IPTG, isopropyl- β -D-thiogalactoside; PL, phospholipid; STB, standard Tris buffer; WT, wild type.

(12), possibly accounting for the significant portion of apoA-IV that exists in a lipid-dissociated state in human plasma (2, 4).

In addition to similarities in predicted secondary structure, apoA-IV is also related to the other apolipoproteins at the genetic level. The human apoA-IV gene is located in the same 15-kb gene complex as apoA-I and apoC-III on the long arm of chromosome 11 (13). In fact, intraexonic duplication of the apoA-I gene has been suggested to have led to the formation of the apoA-IV gene some 300 million years ago (14). Therefore, one might expect that apoA-IV would exhibit tertiary structure similarities to the more extensively studied apoA-I and apoE. Both of these apolipoproteins have been proposed to exhibit a general structural organization that is composed of two functional domains. These domains are composed of clusters of amphipathic helical repeats and play different functional roles within the protein. The best information obtained thus far has come from an X-ray crystallography study of an N-terminal fragment of apoE. This paper shows that the N-terminal 22 kDa of apoE can form a four-helix bundle structure that is relatively stable in the absence of lipid (15). The remaining C-terminal domain exists in a less defined structure that is poised to interact with lipids to trigger an unfolding of the N-terminal domain as the protein associates with lipid. This unfolding event exposes a binding site for the low-density lipoprotein receptor in the N-terminal domain (for a review, see ref 16). Without the benefit of a monomeric, lipid-free crystal structure, it has also been suggested that apoA-I exhibits a similar functional domain organization in solution. Deletion mutagenesis studies have indicated that the N-terminal half of apoA-I is responsible for most of the helical structure and stability in the lipid-free form and that the C-terminal half is less organized. Upon lipid binding, the C-terminal domain undergoes a dramatic increase in helicity and becomes the major stabilizing domain in the lipid-bound state (17, 18). More recent work has further defined these domains and proposed a two-step model for the binding of apoA-I to lipid (19). The weight of the evidence indicates that the N-terminal domain of apoA-I (about residues 1–187) forms a helical bundle structure that is in a molten globular state (20, 21). In contrast, the C terminus (188–243) forms a less organized domain that is required for lipid-binding events (17, 19, 22–25).

Given the similarities between apoA-IV and the relatively well-studied apoA-I and apoE molecules, we hypothesized that a two-functional domain architecture may be a common theme among the exchangeable apolipoproteins and that a similar model would apply to apoA-IV. On this basis, we expected to find: (a) an N-terminal domain composed of associated α helices and a relatively disordered C-terminal region and (b) the lipid-binding functionality of apoA-IV to be localized to the C terminus. In addition, our recent studies have indicated that the class Y character of the extreme C-terminal helix in apoA-I is critical for its interaction with the ABCA1 transporter (25, 26). We speculated that this helix might act as a tether to specific lipid domains on the cell surface, facilitating its interaction with ABCA1 (26). Given that apoA-IV contains a number of class Y helices in its C-terminal half, we further hypothesized that one or more of these helices would be critical for its ability to promote cellular cholesterol efflux via ABCA1.

To test these ideas, we took the approach of deleting discrete domains from each end of apoA-IV and assessing the effects on the structural organization as well as the ability to associate with lipids and promote ABCA1-mediated cholesterol efflux. We found that apoA-IV indeed contains a large domain that may resemble the N-terminal helical bundle structure of apoA-I. However, apoA-IV lacks the strong C-terminal lipid-binding domain. In fact, the extreme C-terminal 44 amino acids appeared to inhibit the molecule from interacting with lipids and promoting cholesterol efflux.

EXPERIMENTAL PROCEDURES

Materials. SDS-PAGE gels were obtained from Bio-Rad (Hercules, CA) or Amersham-Pharmacia (Piscataway, NJ). Primer synthesis and DNA sequencing were performed by the University of Cincinnati DNA Core (Cincinnati, OH). Restriction enzymes were purchased from New England Biolabs (Beverly, MA). Human small intestine QUICK-Clone cDNA was purchased from BD Biosciences Clontech (product 7176-1) (Palo Alto, CA). IgA protease (*Igase*) was purchased from Mobi-Tech (Marco Island, FL). BL-21 (DE3) *Escherichia coli* and the pET30 vector were from Novagen (Madison, WI). Isopropyl- β -D-thiogalactoside (IPTG) was from Fisher Scientific (Pittsburgh, PA). Bis[sulfosuccinimidyl] suberate (BS₃) was purchased from Pierce (Rockford, IL). 1,2-Dimyristoyl-*sn*-glycero-3-phosphatidylcholine (DMPC) was acquired from Avanti Polar Lipids (Birmingham, AL). Fatty-acid-free bovine serum albumin (BSA) was from Calbiochem (San Diego, CA). 8-Bromoadenosine 3':5'-cAMP was from Sigma-Aldrich (St. Louis, MO). Fetal bovine serum, Dulbecco's modified Eagle medium, and phosphate-buffered saline were from Invitrogen Life Technologies (Carlsbad, CA). RAW 264.7 mouse macrophage cells were from American Type Culture Collection (Manassas, VA). All chemicals reagents were of the highest quality available.

Cloning and Mutagenesis of Human apoA-IV. A human small intestine cDNA library was used to clone human apoA-IV. PCR primers were designed to amplify the coding region of human apoA-IV. After amplification, forward- and reverse-flap primers were designed containing an *Nco*I and *Hind*III cleavage site, respectively. The forward primer also contained the sequence encoding for a proteolytic cleavage site specific for *Igase* that is required for removing the histidine tag from the purified protein (27). The apoA-IV DNA was then ligated into the pET30 vector (Novagen) and completely sequenced.

Most of the deletion mutants used wild-type (WT) apoA-IV in the pET30 vector as the template for PCR-based mutagenesis. The Δ 1–39 mutant and Δ 1–61 mutant forward primers were designed similarly to the WT, but instead of the clamp-region nucleotides encoding the N-terminal amino acids, they matched the 40th and 62nd amino acids, respectively. The C-terminal mutations were created by performing PCR-based site-directed mutagenesis (Quick-Change, Novagen) to insert stop codons at specific locations. The N- and C-terminal double mutations were created by inserting stop codons into the Δ 1–39 mutant as their template.

Protein Expression and Purification. To generate WT human apoA-IV, we modified our highly efficient *E. coli*

expression system used previously for human apoA-I (27). The expression construct was transfected into *E. coli* BL-21 cells and grown in Luria–Bertani (LB) culture media that included kanamycin for selection of the pET30 transformants. Protein expression was driven by the T7 promoter upon exposure to IPTG for 2 h. After expression, the bacterial cells were pelleted and lysed by sonication, leaving the recombinant apoA-IV in the supernatant after centrifugation. The presence of the histidine tag allowed for easy purification by using a histidine-binding column (Ni^{2+} -affinity column). The protease Igase was used to cleave the leader portion (with the histidine tag) of the protein, thus leaving the mature form of apoA-IV with an additional Thr-Pro on the N terminus. Finally, the sample was applied to a His-bind column a second time to separate the mature protein from the cleaved tag. ApoA-IV exists in humans as two major isoforms differing at amino acid position 360 (Gln, type I; His, type II) (28). The protein studied in this paper was the type II isoform. However, we have generated the point mutants necessary to convert type II to type I for both the WT protein and the $\Delta 1-61$ deletion mutants (the C-terminal deletions do not contain this site) and compared them using all of the structural and functional assays described below. We found no significant differences between the two isoforms (data not shown).

Circular Dichroism (CD) Spectroscopy. The average secondary structures of the apoA-IV mutants were determined by obtaining CD spectra at room temperature using a Jasco J-600 spectropolarimeter. The α -helix content was calculated from the molar ellipticity at 222 nm, as described (29). The thermal denaturation was monitored from the change in molar ellipticity at 222 nm over the temperature range 20–80°C, as described (30). The cooperativity index, n , describing the sigmoidicity of the thermal denaturation curve and the van't Hoff enthalpy, ΔH_v , were calculated as described previously (19).

Fluorescence Measurements. Fluorescence measurements were carried out with a Hitachi F-4500 fluorescence spectrophotometer at 25 °C. 8-Anilino-1-naphthalenesulfonic acid (ANS) fluorescence spectra were collected from 400 to 600 nm at an excitation wavelength of 395 nm in the presence of 50 $\mu\text{g}/\text{mL}$ protein and an excess of ANS (250 μM) (19).

Self-Association Determination. Lipid-free WT apoA-IV and various mutants were dialyzed into 20 mM sodium phosphate buffer at pH 7.5, containing 20 mM NaCl at a protein concentration of 1 mg/mL. The proteins were then cross-linked by adding 50 mM BS_3 stock in DMSO to a final concentration of 10 mM BS_3 for 1 h at room temperature. The reactions were quenched by adding 1 M Tris-HCl at pH 7.5 to a final concentration of 50 mM for 15 min at room temperature. After quenching, 4 μg of each protein sample were then run on 4–25% gradient polyacrylamide denaturing gels and stained with Coomassie blue (31).

DMPC Liposome Solubilization. DMPC in chloroform was dried in a glass tube and brought up in 1 mL of degassed standard Tris buffer (STB; 10 mM Tris, 0.15 M NaCl, 1 mM EDTA, and 0.2% NaN_3) at a concentration of 5 mg/mL. Multilamellar liposomes were formed by sonication for 30 s with a model 550 sonic dismembrator at level 5 with a microtip (Fisher). The experiments were performed in an Amersham Biosciences Ultraspec 4000 at a constant temperature of 24.5 °C, as maintained by a circulating water

bath. Each protein sample was then added to the liposomes at a mass ratio of 10:1 (weight of DMPC/protein) in separate cuvettes, and the absorbance was recorded over 30 min at 325 nm. The y axis of the graph is the ratio of the absorbance at any given time point (OD) to the initial absorbance at time zero (OD^0) (32).

Cholesterol Efflux Studies. The transformed mouse macrophage cell line RAW264.7 was maintained in growth medium (Dulbecco's modified Eagle medium, 10% fetal bovine serum, and 50 $\mu\text{g}/\text{mL}$ gentamycin). The cells were grown to 70–80% confluency in 48-well plates, and the growth medium was removed. The cells were then labeled with 1.0 $\mu\text{Ci}/\text{mL}$ [^3H] cholesterol in efflux medium (DMEM + 0.2% BSA) with or without 0.3 mM 8-bromo-cAMP for 24 h. After 24 h, the cells were washed twice with PBS, containing 0.2% BSA, and once with efflux medium. Efflux medium, containing differing concentrations of protein acceptors, was added to the wells with or without cAMP for 8 h. After 8 h, 150 μL of sample of efflux medium was removed and filtered through a 0.45- μm filter to remove any floating cells. The amount of [^3H] cholesterol in 100 μL of each sample was then measured by liquid scintillation counting. The percent cholesterol efflux was calculated by dividing the counts in the medium by the total cell counts at time zero minus the cholesterol efflux to media alone at 8 h (26). For the experiments studying the dependence of cholesterol efflux on acceptor protein concentration, estimated " K_m " and " V_{max} " values were obtained by fitting the data to the following equation: $Y = V_{\text{max}}[X/(X + K_m)]$, where Y represents the percent of total cellular cholesterol effluxed per hour and X represents the concentration of acceptor protein present in terms of $\mu\text{g}/\text{mL}$ (33).

RESULTS

As discussed above, we hypothesized apoA-IV would have a modular domain structure based on its sequence similarities to apoE and apoA-I. To test this, we created deletion mutants by cutting from the N- and C-terminal ends of the apoA-IV molecule and then subjected the mutants to a battery of structural and functional assays designed to determine: (a) the region(s) of the highest structural organization and (b) region(s) involved in lipid binding and ABCA1-mediated cholesterol efflux. Figure 1 is a linear diagram of human apoA-IV showing its predicted 22-residue repeats and punctuating proline residues (34, 35). The arrows indicate sites of deletion from both ends of the molecule. For the C-terminal mutations, stop codons were introduced to delete a C-terminal region, which is not predicted to contain amphipathic α helices ($\Delta 333-376$) and subsequently each predicted helical domain was deleted up to amino acid 249. Regions were deleted from the N terminus to remove a predicted nonamphipathic helical domain ($\Delta 1-39$) and then the first predicted N-terminal helical segment ($\Delta 1-61$).

After expression and purification, the proteins were analyzed by SDS–PAGE. The protein preparations were routinely greater than 95% pure as illustrated by the subset of proteins in Figure 2. The majority of the proteins migrated to positions near their predicted molecular weight as determined by the amino acid sequence. However, the $\Delta 1-39$ mutant appeared to be larger than expected (about 43 000 Da as opposed to 39 166 Da) on the gel. We confirmed that

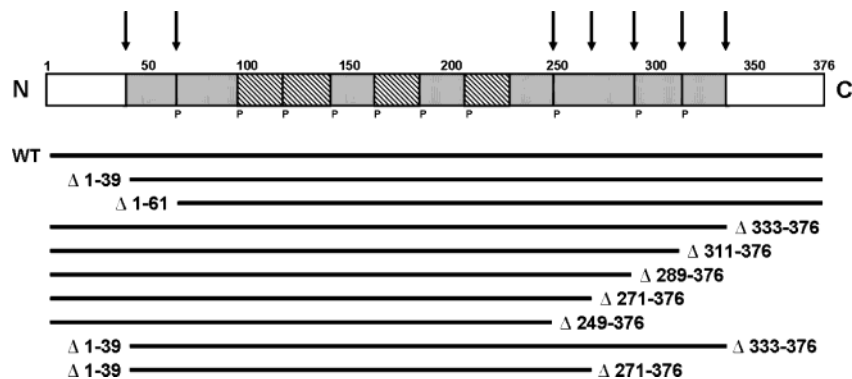


FIGURE 1: Linear diagrams of WT apoA-IV and truncation mutants. The shaded boxes represent predicted class Y amphipathic α helices, and the hatched boxes represent class A helices. Most repeats are punctuated by a proline residue (P) (22). The arrows are placed at sites where deletions were made either in the N or C terminus. Each deletion mutant used in this study is represented by a solid black line showing the sequence that was left intact.

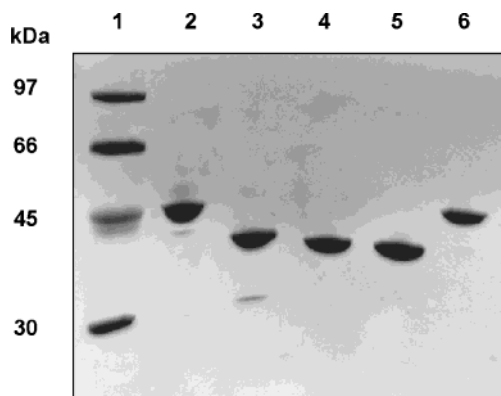


FIGURE 2: SDS-PAGE analysis of WT apoA-IV and representative mutant forms. After expression and purification as described in the Experimental Procedures, 4 μ g samples of apolipoprotein were electrophoresed on an 18% denaturing polyacrylamide gel and stained with Coomassie blue. Lane 1: Amersham-Pharmacia low-molecular-weight marker (cat. 17-0446-01). Lane 2: WT apoA-IV. Lane 3: Δ 333–376. Lane 4: Δ 311–376. Lane 5: Δ 1–61. Lane 6: Δ 1–39.

the mass of this mutant was indeed correct by MALDI mass spectrometry (39 175 Da). Similar inconsistencies in the apparent molecular weight of apoA-IV deletion mutants have been noted previously and may be attributed to decreased SDS binding to particular mutants causing them to migrate slower on the gel (36).

Structural Studies. We next performed a series of structural studies on the proteins. The α -helical content was determined by CD (Table 1). The α -helical content of WT apoA-IV was 40% or roughly 151 helical residues. Removal of the C-terminal amino acids down to residue 271 resulted in little change in the overall helical content. However, for apoA-IV molecules containing deletions past residue 271, we noted a marked decrease in helicity. Interestingly, removing the N-terminal 39 amino acids resulted in a marked decrease in helicity that persisted in all mutants that had this domain deleted.

We next performed thermal denaturation experiments that monitored the helical content of the proteins by CD as a function of temperature. Figure 3A shows that WT apoA-IV remained in a relatively native conformation until about 43 $^{\circ}$ C, where it underwent a rapid denaturation followed by a plateau. This is compared to a denaturation profile for recombinant WT apoA-I. The T_m for apoA-IV is 51 $^{\circ}$ C compared to 60 $^{\circ}$ C for apoA-I, indicating that, on average,

Table 1: Conformation and Stability Properties of WT apoA-IV and the Various Deletion Mutants

	α helix (%) ^a	cooperativity index ^b	T_m^c ($^{\circ}$ C)	ΔH_v^d (kcal/mol)	self-association ^e
WT apoA-IV	40	13.4	51	58	1/2
Δ 333–376	39	12.5	54	52	1/2
Δ 311–376	39	8.8	51	40	1/2
Δ 289–376	44	5.9	46	33	1/2/3/4...
Δ 271–376	41	6.4	47	34	1/2/3/4...
Δ 249–376	28	5.6	44	33	1/2/3/4...
Δ 1–39	31	14.5	54	60	1/2
Δ 1–61	35	13.2	52	56	1/2
Δ 1–39, 333–376	31	16.3	52	68	1/2
Δ 1–39, 271–376	20	5.5	56	28	1/2/3/4...
WT apoA-I	46	7.8	60	33	ND
Δ 190–243 (apoA-I)	57	12.0	56	48	ND

^a Approximate α -helical contents determined from the molar ellipticity at 222 nm at 25 $^{\circ}$ C as calculated according to Chen et al. (47). Each value represents the average of at least two observations. Typical standard deviations for these experiments are $\pm 5\%$. ^b Describes the sigmoidicity of the thermal denaturation curve (see the Experimental Procedures). Each value represents the average of at least two observations. ^c Midpoint temperature of denaturation. Typical reproducibility for these experiments is ± 2.0 $^{\circ}$ C (19). ^d Estimated error on these experiments is ± 0.5 kcal/mol. ^e Qualitative estimation of the oligomerization behavior of the mutants as assessed by BS³ cross-linking studies. A value of 1/2 indicates the presence of monomers and dimers (typically about 70% dimer and 30% monomer). A value of 1/2/3/4... indicates the presence of a relatively even distribution of multiple oligomers.

the α helices in apoA-IV are significantly less stable. The sigmoidicity of the apoA-I denaturation curve is significantly less than that for apoA-IV. A cooperativity index that describes the sigmoidal nature of the denaturation is listed in Table 1 along with the midpoint temperature and the van't Hoff enthalpy of the denaturation. Removal of C-terminal residues 333–376 stabilized the protein slightly ($T_m = 54$ $^{\circ}$ C versus 51 $^{\circ}$ C) and had relatively minimal effects on the cooperativity index and van't Hoff enthalpy. The properties of Δ 333–376 were similar to the proposed N-terminal, single-domain helix bundle structure formed by residues 1–190 of apoA-I. Removal of the 22-residue helix spanning residues 311–333 disrupted the organization of the apoA-IV molecule, as indicated by much larger reductions in the cooperativity and van't Hoff enthalpy. As more extensive deletions of the C terminus were made (parts A and B of Figure 3), the cooperativity decreased to a minimum of about 6 with similar reductions for the T_m and ΔH_v . At the N

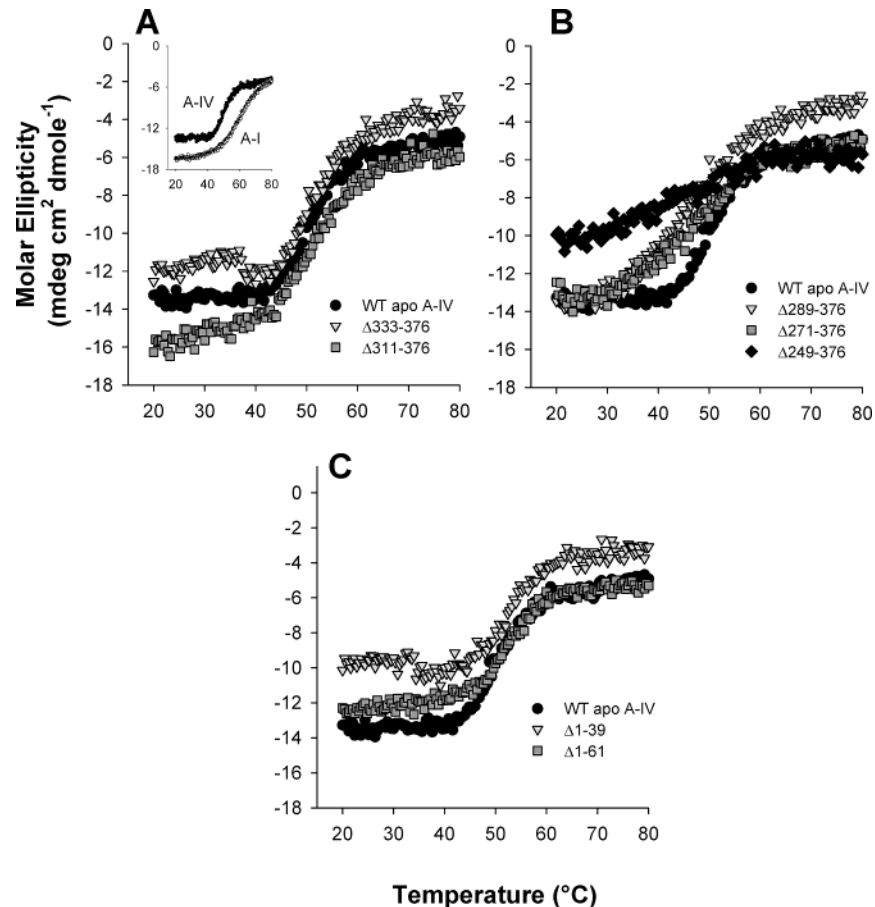


FIGURE 3: Thermal unfolding of N- and C-terminal mutants of apoA-IV. Thermal unfolding was monitored by ellipticity at 222 nm. (A) WT apoA-IV (●), $\Delta 333-376$ (▼) and $\Delta 311-376$ (■). The inset shows WT apoA-IV compared to human apoA-I. (B) WT apoA-IV (●), $\Delta 289-376$ (▼), $\Delta 271-376$ (■) and $\Delta 249-376$ (◆). (C) WT apoA-IV (●), $\Delta 1-39$ (▼) and $\Delta 1-61$ (■).

terminus, deleting amino acids 1–39 or 1–61 had little effect on cooperativity, T_m , and van't Hoff enthalpy as compared to those of the WT (Figure 3C and Table 1). Thus, it appeared that removing the extreme ends of the molecule (1–61 or 333–376) preserved the general structure adopted by the WT protein; however, further deletions into the C-terminal end clearly disrupted the protein organization. It should be noted that we attempted to make further deletions into the N terminus ($\Delta 1-83$, $\Delta 1-94$, and $\Delta 1-138$). However, these deletions resulted in mutant proteins that were quickly degraded during the purification from our bacterial expression system (data not shown). We believe that these mutations caused catastrophic perturbations of the tertiary structure, exposing numerous sites that were normally buried within the protein to proteolytic degradation.

Double mutants were also created with deletions at both the N and C termini. The first mutant was designed to remove amino acids 1–39 and 333–376, which are not thought to form class A or Y amphipathic helices (Figure 1). A second mutant was then designed to include amino acids 40–270. Figure 4 and Table 1 show that $\Delta 1-39$ 333–376 exhibited similar, if not increased, stability parameters to the WT, but the structure of $\Delta 1-39$ 271–376 was sufficiently perturbed that it did not undergo cooperative unfolding. Thus, the highest cooperativity of unfolding was consistently noted for the intact domain represented by residues 40–332.

As an additional measure of structural organization, we examined the interaction of ANS with the mutants. ANS binds to exposed hydrophobic surfaces resulting in increased

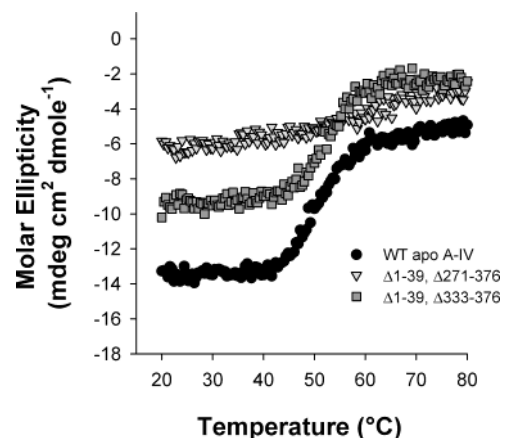


FIGURE 4: Thermal unfolding of combined N- and C-terminal mutants. WT apoA-IV (●), $\Delta 1-39$ 271–376 (▼) and $\Delta 1-39$ 333–376 (■).

fluorescence emission (37). Therefore, the more exposed the hydrophobic domains, the higher the degree of ANS binding and fluorescence. Figure 5 shows the effects of interaction with WT apoA-IV, WT apoA-I, and the various deletion mutants on ANS fluorescence. WT apoA-IV induced much less ANS fluorescence per amino acid as compared to apoA-I. Similar to the thermal denaturation studies, removing amino acids 1–61 or amino acids 333–376 had relatively minor effects on ANS fluorescence as compared to that of WT apoA-IV. $\Delta 311-376$ also exhibited low ANS fluorescence. However, further deletions into the C-terminal end

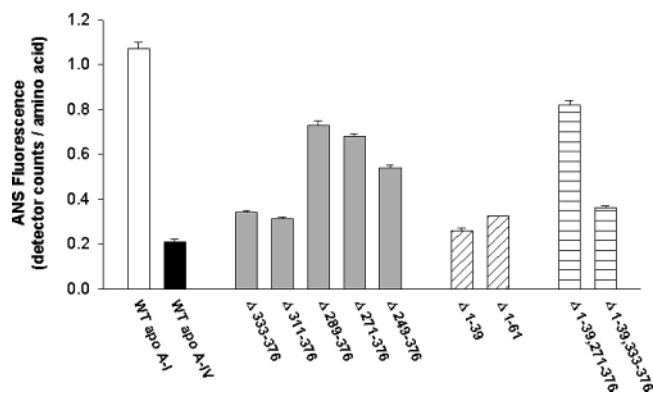


FIGURE 5: Effects of apoA-I, WT apoA-IV, and mutant forms of apoA-IV on ANS fluorescence. A total of 50 $\mu\text{g}/\text{mL}$ protein was added to an excess of ANS (250 μM), and the fluorescence spectra were collected from 400 to 600 nm at an excitation wavelength of 395 nm. The data are reported as detector counts per amino acid measured at the wavelength of maximum fluorescence (484 nm). The values for human apoA-I are shown for comparison.

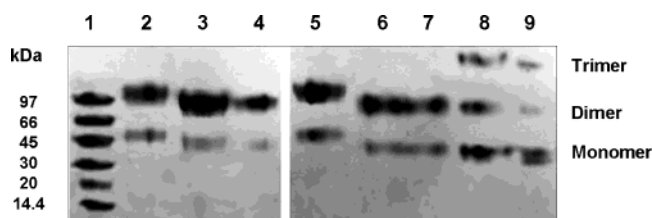


FIGURE 6: SDS-PAGE analysis of the self-association of WT apoA-IV and representative mutant forms. Lipid-free samples were cross-linked in 20 mM PBS with 10 mM BS_3 for 60 min at room temperature. After quenching, 4 μg protein samples were run on 4–25% gradient polyacrylamide denaturing gel and stained with Coomassie blue. Lane 1: Amersham-Pharmacia low-molecular-weight marker. Lane 2: WT apoA-IV. Lane 3: $\Delta 1-39$. Lane 4: $\Delta 1-61$. Lane 5: WT apoA-IV. Lane 6: $\Delta 333-376$. Lane 7: $\Delta 311-376$. Lane 8: $\Delta 289-376$. Lane 9: $\Delta 271-376$.

resulted in dramatic increases in ANS fluorescence. Consistent with the results from the denaturation studies, the double mutant, $\Delta 1-39$ 333–376, exhibited similar ANS fluorescence to the WT, but $\Delta 1-39$ 271–376 was markedly increased. In general, the ANS fluorescence results suggest that the domain-spanning residues 40–332 can fold into a structure that exhibits minimal exposure of hydrophobic residues.

Functional Studies. We next determined the effects of the deletions on several indices of apoA-IV function *in vitro*. Because self-association is a common feature of lipid-free apolipoproteins, the ability of apoA-IV and its deletion mutants to oligomerize was determined by cross-linking with BS_3 . Figure 6 is an SDS-PAGE analysis of protein samples cross-linked at 1 mg/mL. In the case of WT apoA-IV, approximately 70% of the protein was present as a dimer with the remaining 30% as a monomer. Removal of the N-terminal amino acids 1–61 and removal of C-terminal amino acids up to 311–376 did not affect the oligomerization pattern as compared to that of the WT. However, further deletions into the C terminus resulted in an even distribution between the monomer, dimer, and trimer. Both double mutants followed their C-terminal mutant counterpart with $\Delta 1-39$ 333–376 forming only the monomer and dimer and $\Delta 1-39$ 271–376 forming the monomer, dimer, and trimer (data not shown).

To determine the regions of apoA-IV that are important in lipid binding and reorganization, a DMPC lipid clearance assay was performed. In this assay, DMPC multilamellar liposomes are generated in buffer, resulting in a turbid solution. Protein samples are then added, and the turbidity clears as the protein binds and reorganizes the liposomes into discoidal structures. Figure 7 shows that WT apoA-IV cleared the liposomes more slowly than WT apoA-I but clearly was able to reorganize the lipid to some extent. Surprisingly, removal of regions from the C terminus dramatically increased the rate of clearance, contrary to the effect of C-terminal deletion on the ability of apoA-I to clear DMPC liposomes (26). In fact, the increase in lipid clearance was so profound that we were forced to modify our usual protocol from a 2.5:1 (weight of phospholipid/protein) to a 10:1 ratio to slow the reaction to a point at which the kinetics could be measured accurately. The highly increased ability of the C-terminal truncation mutants persisted when the proteins were compared on an equal protein molar basis as well as on a mass basis (data not shown). On the other hand, removal of N-terminal amino acids 1–39 or 1–61 did not affect lipid clearance in the apoA-IV mutants. Interestingly, the N- and C-terminal double mutants did not differ from the WT, despite lacking the same C-terminal amino acids that resulted in the dramatic increase in the C-terminus only mutants.

Similar to apoA-I, apoA-IV has been shown to have the ability to promote the efflux of cholesterol via the ABCA1 pathway (9). We took advantage of our deletion mutants to determine if a particular domain in apoA-IV is responsible for interaction with ABCA1. We used RAW264 macrophages in these studies because it has been clearly established that the addition of cAMP to the cells causes an increase in ABCA1 at the cell surface (38, 39). After treatment of the cells for 24 h with labeled cholesterol and cAMP, lipid-free protein acceptors were added for 8 h to determine their ability to promote cholesterol efflux by the ABCA1-mediated pathway. Figure 8 shows ABCA1-mediated cholesterol efflux over a range of concentrations of WT apoA-IV, the deletion mutants, and WT apoA-I. The apparent K_m and V_{max} values for each of the lipid-free protein acceptors are also given in Table 2. These results show that all proteins tested exhibited generally similar maximum capacities (V_{max}) for ABCA1-mediated cholesterol efflux under these conditions. However, large differences in apparent K_m existed between the proteins; much more WT apoA-IV was required to reach its maximum effect compared to that of apoA-I. However, removal of any of the C-terminal regions resulted in a markedly lower K_m than that for WT apoA-IV and a value that was similar to that of WT apoA-I. In contrast, removal of the N-terminal amino acids 1–39 or 1–61 caused smaller reductions in K_m . The double mutant, $\Delta 1-39$ 271–376 exhibited a lower K_m than that of the WT and was similar to the rest of the C-terminal mutants. In general, the presence of the region 333–376 dramatically diminished the ability of apoA-IV to promote cholesterol efflux via the ABCA1 pathway.

DISCUSSION

On the basis of previous studies of apoE and apoA-I, we anticipated that apoA-IV might exhibit a two-domain structure comprising an N-terminal domain folded into a bundle of 22-residue amphipathic α helices and a relatively dis-

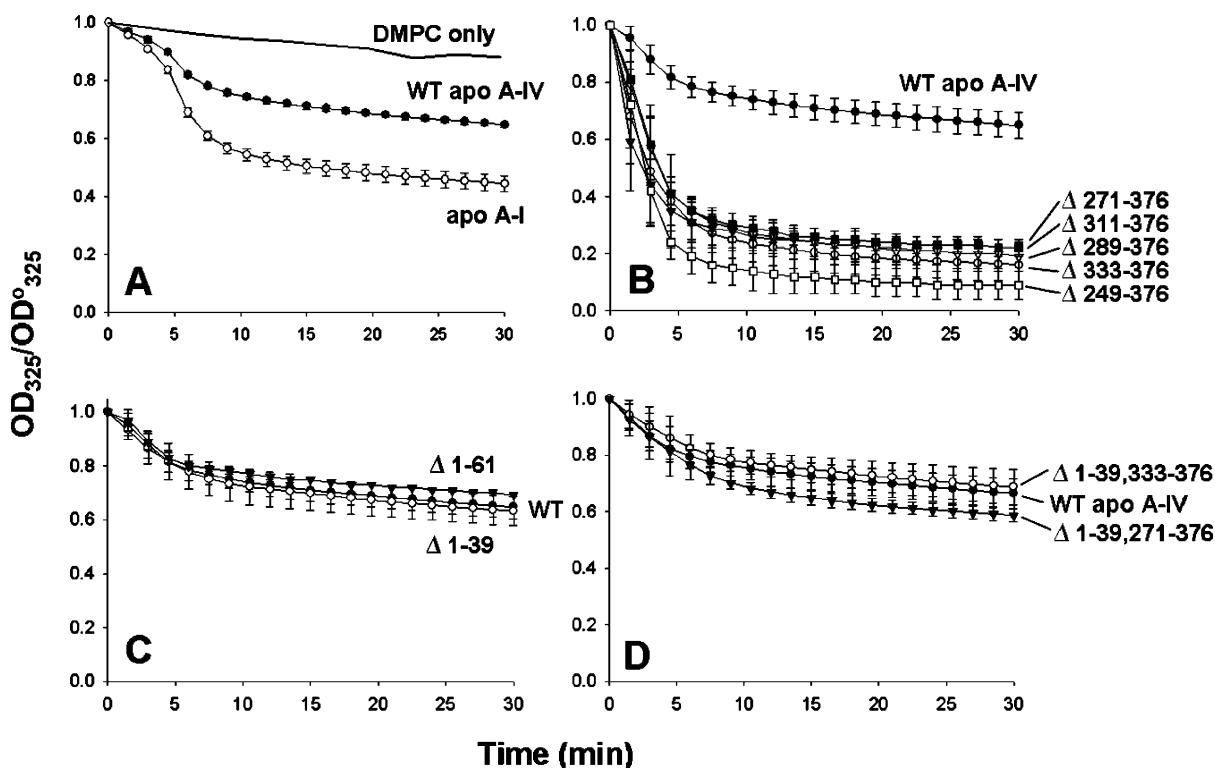


FIGURE 7: DMPC liposome solubilization by apoA-I, apoA-IV, and deletion mutants of apoA-IV. DMPC multilamellar liposomes in STB were maintained at 24.5 °C by a water bath and monitored at 325 nm for 30 min after protein was added (see the Experimental Procedures). (A) WT apoA-IV versus apoA-I. (B) WT apoA-IV versus all of the C-terminal deletion mutants. (C) WT apoA-IV versus the N-terminal deletion mutants. (D) WT apoA-IV versus the combined N- and C-terminal deletion mutants. The y axis is the ratio of the absorbance at 325 nm at any given time point (OD_{325}/OD^0_{325}) (32).

ordered C-terminal domain responsible for lipid interactions. This was reasonable considering the evolutionary and predicted secondary structural similarities between these proteins and the fact that the most C-terminal amphipathic repeat in apoA-IV is a class Y helix with a similar mean residue hydrophobic moment (34) to the lipid binding/cholesterol-effluxing helical domain identified in apoA-I (26). While we found evidence that apoA-IV contains at least one large domain (residues 40–332) comprising about 77% of the amino acid sequence, the region(s) of the apoA-IV molecule primarily involved in DMPC clearance and in ABCA1-mediated cholesterol efflux was not located in the C-terminal $1/3$ of the protein. Indeed, removal of the C-terminal nonamphipathic helical domain (residues 333–376) of apoA-IV resulted in the opposite effect of *increased* DMPC clearance and cholesterol efflux. This suggests that there is another sequence within apoA-IV that is responsible for lipid binding and that the C-terminal domain may inhibit it. The effects of the deletions performed in this study on the apoA-IV structure and function are summarized graphically in Figure 9. We discuss these observations in detail below.

ApoA-IV Structure. Our data indicate that apoA-IV exists as a single cooperative domain between residues 40–332. Inspection of Figure 1 shows that this region encompasses about 9 of the potential 22-mer helical repeats that are predicted for the protein. However, our CD data in Table 1 for the mutant $\Delta 1-39$ 333–376 indicates that the domain is only about $1/3$ helical, suggesting that the domain contains an average of about 91 helical amino acids, roughly four 22-mer helices or perhaps a higher number of shorter helices.

Based on the structures of other lipid-free apolipoproteins, it follows that the hydrophobic faces of these helical domains are likely clustered together in the interior of the protein. Such a four-helix bundle structure has been established for the N-terminal domain of apoE (15). In this case, the four-helix bundle has a well-defined secondary and tertiary structure and is stabilized by strong hydrophobic forces and intrahelical salt-bridge interactions, explaining its relatively high free energy of stabilization of about 10 kcal/mol (15). In contrast, the helical bundle in apoA-I is significantly less stable with a free energy of stabilization of about 2–3 kcal/mol (40). This domain likely differs from a classical four-helix bundle in that it is more dynamic with secondary structural elements that do not maintain stable tertiary interactions. This melted tertiary structure is characteristic of molten globule proteins (20). The conformational dynamics of lipid-free apoA-I are evident when it is visualized on a native polyacrylamide gel; it runs as a diffuse or smeared band that is much larger than predicted by its molecular weight (data not shown). ApoA-IV is even less stable than apoA-I as shown in Table 1 and by the fact that it is completely denatured in about 0.5 M guanidine HCl with a calculated free energy of stabilization of less than 1 kcal/mol (41). Despite this low stability, our data indicate that the structure of the domain is highly cooperative and organized in such a way as to efficiently sequester hydrophobic residues within the interior of the protein molecule. This high level of organization is consistent with the fact that monomeric lipid-free apoA-IV runs as a tightly focused band on a native polyacrylamide gel (data not shown). The precise reason for the dichotomy between low stability and

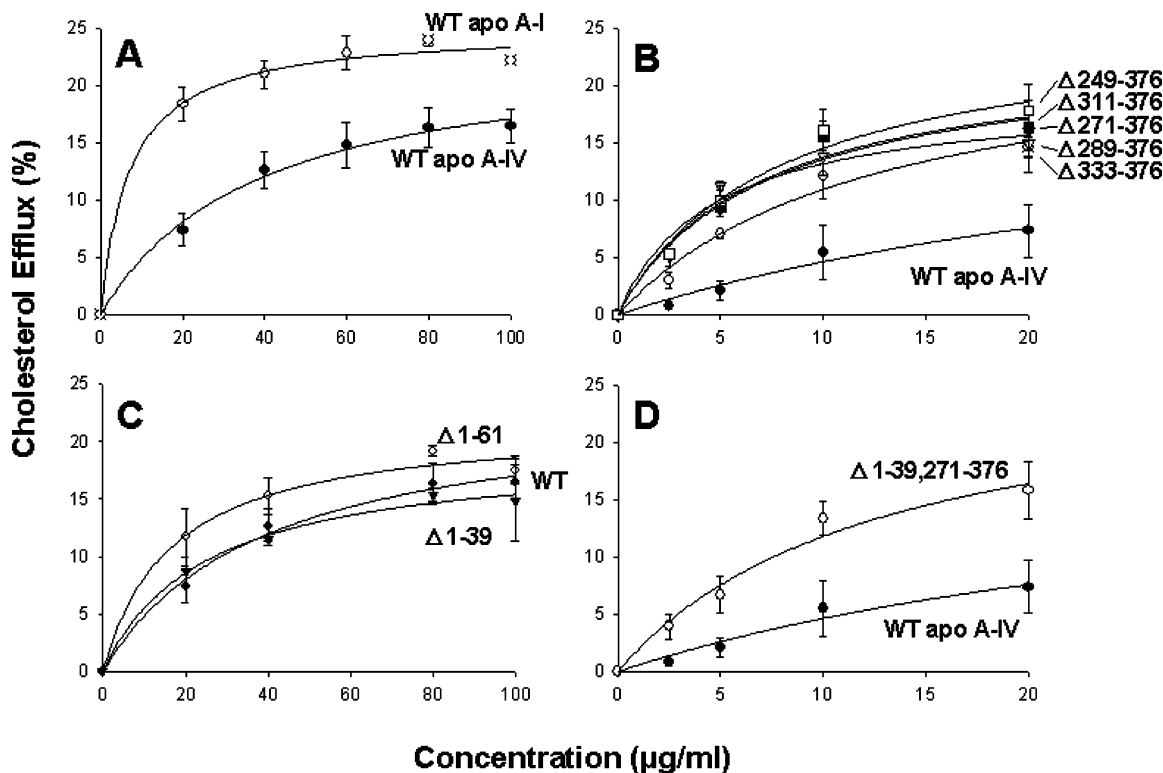


FIGURE 8: ABCA1-mediated cholesterol efflux from RAW264 macrophages. Cells were grown to 70–80% confluency in 48-well plates and labeled for 24 h with [3 H] cholesterol along with 0.3 mM 8-bromo-cAMP to upregulate ABCA1. Protein acceptors at different concentrations were added in DMEM media with 0.2% BSA and 0.3 mM cAMP. After 8 h, samples were counted in a scintillation counter. (A) compares WT apoA-IV and apoA-I. (B) compares WT apoA-IV, Δ 333–376, Δ 311–376, Δ 271–376, and Δ 249–376. (C) compares WT apoA-IV, Δ 1–39, and Δ 1–61. (D) compares WT apoA-IV and the double mutant Δ 1–39, 271–376. Note: the concentration ranges differ between A and C versus B and D to more effectively show the differing apparent K_m values among the mutants. The data were fit to a simple Michaelis–Menten equation (see the Experimental Procedures) and are shown by the solid lines.

Table 2: Kinetic Parameters for Cholesterol Efflux from RAW264 Macrophages to Lipid-free apoA-IV and Its Deletion Mutants

	K_m^a	V_{max}^b		K_m^a	V_{max}^b
WT apoA-IV	54	3.0	Δ 1–39	26	2.4
Δ 333–376	11	3.2	Δ 1–61	23	2.5
Δ 311–376	8	3.0	Δ 1–39, 333–376	NA ^c	NA
Δ 289–376	5	2.4	Δ 1–39, 271–376	13	3.4
Δ 271–376	7	3.0	WT apoA-I	7	3.1
Δ 249–376	8	3.2			

^a Concentration of acceptor apolipoprotein at 50% of the maximal rate of cholesterol efflux (V_{max}). The units are micrograms of apolipoprotein per milliliter of media. Typical error is approximately 14% of the mean value. ^b Maximal rate of cholesterol efflux (percent of total cellular cholesterol label per hour) calculated as described in the Experimental Procedures. Typical error is approximately 36% of the mean value. ^c This mutant did not exhibit saturable cholesterol efflux kinetics and could not be subjected to analysis.

high structural organization cannot be directly addressed by our studies. However, we propose that, compared to apoA-I and apoE, the stabilizing forces within apoA-IV may be dominated less by hydrophobic forces acting upon sequestered nonpolar residues and more by hydrophilic interactions among exposed polar residues. Indeed, the helical repeats within apoA-IV are, on average, less hydrophobic and have a smaller hydrophobic helical wedge angle than the helices in the other apolipoproteins (12). Such polar interactions on the surface may result in a delicate but defined tertiary structure for apoA-IV.

We should point out that our results differ from previous studies of internal deletion mutants of apoA-IV. Studies by

Weinberg et al. (32, 42) and Emmanuel et al. (36) demonstrated that all internal deletions of various regions of apoA-IV, including areas that are outside of the 40–332 domain proposed here, resulted in major reductions in the thermal stability of apoA-IV. However, the mutants utilized in these studies contained a hydrophobic decapeptide tag on the N terminus that was demonstrated to affect both structural and functional aspects of the protein (42). It may be that the presence of the tag region made the mutants much more sensitive to destabilizations from deletions than seen in the current study in which the purification tag had been removed. In any case, the general result from both studies is consistent with the notion that lipid-free apoA-IV is composed of a large domain that is relatively organized but unstable.

Functional Studies. An important function of the exchangeable apolipoproteins is to bind to lipid to form lipoproteins. We compared the ability of WT apoA-IV to clear DMPC liposomes to that of apoA-I. This assay measures the end result of a complex, multistep interaction between proteins and lipids (see the reaction scheme in Segall et al. in ref 43). Although the assay does not speak directly to lipid-binding affinity per se, it does offer a general index of the overall ability of a protein to solubilize a planar lipid surface into lipoprotein-like particles. In agreement with studies by Weinberg et al. (32), apoA-IV was less efficient than apoA-I at clearing lipids in the DMPC assay. However, when we removed the extreme C-terminal region (amino acids 333–376), the ability apoA-IV to clear DMPC increased strikingly. Further deletions into the C-terminal end, including our most extreme mutation Δ 249–376, did





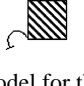
	Mutation	Lipid clearance	Comment
	WT	Slow	Lipid binding region MASKED, Helical bundle domain INTACT.
	ΔN to 39	Slow	Lipid binding region DISRUPTED, Helical bundle domain INTACT.
	ΔC to 333	Fast	Lipid binding region EXPOSED, Helical bundle domain INTACT.
	ΔC past 333	Fast	Lipid binding region EXPOSED, Helical bundle domain DISRUPTED.
	ΔC to 333 <u>and</u> ΔN to 39	Slow	Lipid binding region DISRUPTED, Helical bundle domain INTACT.

FIGURE 9: Generalized model for the effects of deletions on the structure and function of lipid-free apoA-IV. The hatched square represents the correctly folded, large structural domain (a bundle of 22-mer amphipathic α helices punctuated by prolines) that is postulated to exist in lipid-free apoA-IV. The irregular shape with the wavy lines represents a major disruption in the stability and cooperativity of this domain. The small white square on the N terminus represents a putative lipid-binding domain that is masked by the C-terminal 44 amino acid region in the WT protein (see text). The relative rates of lipid clearance refer to DMPC clearance rates relative to the WT apoA-IV (defined as “slow”) versus the Δ 333–376 deletion mutant (defined as “fast”), see Figure 7.

not alter this increased clearance. This is in direct contrast to the case of apoA-I, where deletion of the final helix resulted in dramatically *decreased* DMPC clearance efficiency (17, 19). Removing amino acids 1–39 from WT apoA-IV had no effect on lipid clearance (Figure 7C) but dramatically decreased the ability of mutants lacking residues 271–336 or 333–376 to solubilize DMPC liposomes (parts B and D of Figure 7). These results suggest that residues 1–39 within apoA-IV can mediate DMPC clearance efficiently, but in the presence of the C-terminal 44 amino acids, this site is masked (Figure 9). Removal of the C-terminal domain may either unmask this site or allow a conformational change that brings it to bear on the target lipid surface. Whether this N-terminal region is the actual site of lipid binding or if perturbations within this domain affect a more distally located functional domain is unclear and will require further study.

Both apoA-IV and apoA-I are acceptors in ABCA1-mediated cholesterol efflux *in vitro*. Figure 8 and Table 2 show that apoA-IV and apoA-I have similar V_{\max} values for ABCA1-mediated cholesterol efflux, but apoA-IV is less efficient, exhibiting a higher K_m value. However, similar to DMPC binding, the removal of the C-terminal 44 amino acids increased the ability of apoA-IV to promote cholesterol efflux by reducing the K_m to a value comparable to that of apoA-I. Further C-terminal deletions had similar effects, presumably because they caused disruption of the helix bundle exposing 22-residue amphipathic α helices (see the increased ANS fluorescence in Figure 5). In terms of the identity of a recognition site within apoA-IV, it has been suggested that a particular array of acidic residues across two amphipathic helices in the C terminus of apoA-I is required to promote ABCA1-mediated cholesterol efflux (44). Our analysis shows that the helical domains between amino acids 150 and 193 in apoA-IV appear to fit this criterion, whereas those closer to the C terminus do not. Future studies will be aimed at determining if this domain

is responsible for mediating the interaction of apoA-IV in the absence of the C terminus. Intriguingly, the double mutant Δ 1–39, 271–376 that cleared lipids slowly (Figure 7D), was still efficient at promoting cholesterol efflux (Figure 8D). This suggests that different sites within the apoA-IV molecule may be required for the two functions.

We would emphasize two implications of this paper concerning the functionality of apoA-IV. First, we have demonstrated that there are sequences within apoA-IV that are clearly capable of mediating apoA-I-like functions, such as lipid binding and cholesterol efflux. However, the C-terminal nonamphipathic helical sequence can attenuate these functions. Of interest is the fact that this C-terminal region 333–376 contains a unique sequence that is composed of a high concentration of glutamine and glutamate residues. Of the C-terminal 25 amino acids of human apoA-IV, 11 are glutamine and 6 are glutamate. Because there is no homologue of this sequence in any of the other exchangeable apolipoproteins, it is tempting to speculate that this “Gln/Glu-rich” region may have interesting functional ramifications for apoA-IV. More focused deletion studies will be required to test this hypothesis in the future. Weinberg et al. have proposed that this region may be an evolutionary innovation that imparted a role for apoA-IV in chylomicron assembly and secretion around the time of the divergence of mammals and avians (45). On the basis of our data, we would propose that this domain may also have evolved to allow apoA-IV to perform additional functions that are distinct from the other exchangeable apolipoproteins by suppressing its apoA-I-like properties. Indeed, the protein has been implicated as a circulating satiety factor along with its roles in lipid metabolism (46). This may also account for observations that apoA-IV may exist in the lipid-free form to a much greater extent in plasma versus apoA-I or apoE (4). However, it should be noted that the presence or absence of a variant of the “Gln/Glu-rich” sequence does not necessarily correlate with the ability of apoA-IV to disrupt

lipids. For example, chicken apoA-IV, which lacks the sequence, appears to disrupt DMPC liposomes with similar kinetics as human apoA-IV (45). Second, it is clear that apoA-IV does not possess the C-terminal lipid-binding functional domain that is present in apoA-I and apoE. This is the case even in the absence of the inhibitory C-terminal 44 amino acids. Although apoA-IV may have evolved from gene duplication events of ancestral apolipoproteins and shares the basic amphipathic helical building blocks, the overall localization of functional domains within the sequence is quite different from apoA-I and apoE. Clearly, more work is warranted to fully understand the functional consequences of this distinct structural organization.

REFERENCES

- Swaney, J. B., Reese, H., and Eder, H. A. (1974) Polypeptide composition of rat high-density lipoprotein: Characterization by SDS-gel electrophoresis, *Biochem. Biophys. Res. Commun.* **59**, 513–519.
- Hayashi, H., Nutting, D. F., Fujimoto, K., Cardelli, J. A., Black, D., and Tso, P. (1990) Transport of lipid and apolipoproteins A-I and A-IV in intestinal lymph of the rat, *J. Lipid Res.* **31**, 1613–1625.
- Tso, P., Liu, M., Kalogeris, T. J., and Thomson, A. B. (2001) The role of apolipoprotein A-IV in the regulation of food intake, *Annu. Rev. Nutr.* **21**, 231–254.
- Green, P. H., Glickman, R. M., Riley, J. W., and Quinet, E. (1980) Human apolipoprotein A-IV. Intestinal origin and distribution in plasma, *J. Clin. Invest.* **65**, 911–919.
- Fujimoto, K., Fukagawa, K., Sakata, T., and Tso, P. (1993) Suppression of food intake by apolipoprotein A-IV is mediated through the central nervous system in rats, *J. Clin. Invest.* **91**, 1830–1833.
- Okumura, T., Fukagawa, K., Tso, P., Taylor, I. L., and Pappas, T. N. (1996) Apolipoprotein A-IV acts in the brain to inhibit gastric emptying in the rat, *Am. J. Physiol.* **270**, G49–G53.
- Lefevre, M., and Roheim, P.S. (1984) Metabolism of apolipoprotein A-IV. [Review] [46 refs], *J. Lipid Res.* **25**, 1603–1610.
- Ostos, M. A., Conconi, M., Vergnes, L., Baroukh, N., Ribalta, J., Girona, J., Caillaud, J. M., Ochoa, A., and Zakin, M. M. (2001) Antioxidative and antiatherosclerotic effects of human apolipoprotein A-IV in apolipoprotein E-deficient mice, *Arterioscler., Thromb., Vasc. Biol.* **21**, 1023–1028.
- Remaley, A. T., Stonik, J. A., Demosky, S. J., Neufeld, E. B., Bocharov, A. V., Vishnyakova, T. G., Eggerman, T. L., Patterson, A. P., Duverger, N. J., Santamarina-Fojo, S., and Brewer, H. B., Jr. (2001) Apolipoprotein specificity for lipid efflux by the human ABCA1 transporter, *Biochem. Biophys. Res. Commun.* **280**, 818–823.
- Steinmetz, A., and Utermann, G. (1985) Activation of lecithin: cholesterol acyltransferase by human apolipoprotein A-IV, *J. Biol. Chem.* **260**, 2258–2264.
- Boguski, M. S., Elshourbagy, N., Taylor, J. M., and Gordon, J. I. (1985) Comparative analysis of repeated sequences in rat apolipoproteins A-I, A-IV, and E, *Proc. Natl. Acad. Sci. U.S.A.* **82**, 992–996.
- Weinberg, R. B. (1987) Differences in the hydrophobic properties of discrete α -helical domains of rat and human apolipoprotein A-IV, *Biochim. Biophys. Acta* **918**, 299–303.
- Karathanasis, S. K. (1985) Apolipoprotein multigene family: Tandem organization of human apolipoprotein AI, CIII, and AIV genes, *Proc. Natl. Acad. Sci. U.S.A.* **82**, 6374–6378.
- Karathanasis, S. K., Oettgen, P., Haddad, I. A., and Antonarakis, S. E. (1986) Structure, evolution, and polymorphisms of the human apolipoprotein A4 gene (APOA4), *Proc. Natl. Acad. Sci. U.S.A.* **83**, 8457–8461.
- Wilson, C., Wardell, M. R., Weisgraber, K. H., Mahley, R. W., and Agard, D. A. (1991) Three-dimensional structure of the LDL receptor-binding domain of human apolipoprotein E, *Science* **252**, 1817–1822.
- Weisgraber, K. H. (1994) Apolipoprotein E: Structure–function relationships. [Review] [201 refs], *Adv. Protein Chem.* **45**, 249–302.
- Davidson, W. S., Hazlett, T., Mantulin, W. W., and Jonas, A. (1996) The role of apolipoprotein AI domains in lipid binding, *Proc. Natl. Acad. Sci. U.S.A.* **93**, 13605–13610.
- Oda, M. N., Forte, T. M., Ryan, R. O., and Voss, J. C. (2003) The C-terminal domain of apolipoprotein A-I contains a lipid-sensitive conformational trigger, *Nat. Struct. Biol.* **10**, 455–460.
- Saito, H., Dhanasekaran, P., Nguyen, D., Holvoet, P., Lund-Katz, S., and Phillips, M. C. (2003) Domain structure and lipid interaction in human apolipoproteins A-I and E, a general model, *J. Biol. Chem.* **278**, 23227–23232.
- Gursky, O., and Atkinson, D. (1996) Thermal unfolding of human high-density apolipoprotein A-I: Implications for a lipid-free molten globular state, *Proc. Natl. Acad. Sci. U.S.A.* **93**, 2991–2995.
- Rogers, D. P., Roberts, L. M., Lebowitz, J., Engler, J. A., and Brouillette, C. G. (1998) Structural analysis of apolipoprotein A-I: Effects of amino- and carboxy-terminal deletions on the lipid-free structure, *Biochemistry* **37**, 945–955.
- Segrest, J. P., Jones, M. K., De Loof, H., Brouillette, C. G., Venkatachalapathi, Y. V., and Anantharamaiah, G. M. (1992) The amphipathic helix in the exchangeable apolipoproteins: A review of secondary structure and function. [Review], *J. Lipid Res.* **33**, 141–166.
- Schmidt, H. H., Remaley, A. T., Stonik, J. A., Ronan, R., Wellmann, A., Thomas, F., Zech, L. A., Brewer, H. B., Jr., and Hoeg, J. M. (1995) Carboxyl-terminal domain truncation alters apolipoprotein A-I in vivo catabolism, *J. Biol. Chem.* **270**, 5469–5475.
- Ji, Y., and Jonas, A. (1995) Properties of an N-terminal proteolytic fragment of apolipoprotein AI in solution and in reconstituted high-density lipoproteins, *J. Biol. Chem.* **270**, 11290–11297.
- Gillotte, K. L., Zaiou, M., Lund-Katz, S., Anantharamaiah, G. M., Holvoet, P., Dhoest, A., Palgunachari, M. N., Segrest, J. P., Weisgraber, K. H., Rothblat, G. H., and Phillips, M. C. (1999) Apolipoprotein-mediated plasma membrane microsolubilization. Role of lipid affinity and membrane penetration in the efflux of cellular cholesterol and phospholipid, *J. Biol. Chem.* **274**, 2021–2028.
- Panagotopoulos, S. E., Witting, S. R., Horace, E. M., Hui, D. Y., Maiorano, J. N., and Davidson, W. S. (2002) The role of apolipoprotein A-I helix 10 in apolipoprotein-mediated cholesterol efflux via the ATP-binding cassette transporter ABCA1, *J. Biol. Chem.* **277**, 39477–39484.
- Panagotopoulos, S. E., Witting, S. R., Horace, E. M., Nicholas, M. J., and Sean, D. W. (2002) Bacterial expression and characterization of mature apolipoprotein A-I, *Protein Expression Purif.* **25**, 353–361.
- Kamboh, M. I., and Ferrell, R. E. (1987) Genetic studies of human apolipoproteins. I. Polymorphism of apolipoprotein A-IV, *Am. J. Hum. Genet.* **41**, 119–127.
- Sparks, D. L., Phillips, M. C., and Lund-Katz, S. (1992) The conformation of apolipoprotein A-I in discoidal and spherical recombinant high-density lipoprotein particles. ¹³C NMR studies of lysine ionization behavior, *J. Biol. Chem.* **267**, 25830–25838.
- Acharya, P., Segall, M. L., Zaiou, M., Morrow, J., Weisgraber, K. H., Phillips, M. C., Lund-Katz, S., and Snow, J. (2002) Comparison of the stabilities and unfolding pathways of human apolipoprotein E isoforms by differential scanning calorimetry and circular dichroism, *Biochim. Biophys. Acta* **1584**, 9–19.
- McGuire, K. A., Davidson, W. S., and Jonas, A. (1996) High yield overexpression and characterization of human recombinant proapolipoprotein A-I, *J. Lipid Res.* **37**, 1519–1528.
- Weinberg, R. B., Anderson, R. A., Cook, V. R., Emmanuel, F., Deneffe, P., Hermann, M., and Steinmetz, A. (2000) Structure and interfacial properties of chicken apolipoprotein A-IV, *J. Lipid Res.* **41**, 1410–1418.
- Davidson, W. S., Gillotte, K. L., Lund-Katz, S., Johnson, W. J., Rothblat, G. H., and Phillips, M. C. (1995) The effect of high-density lipoprotein phospholipid acyl chain composition on the efflux of cellular free cholesterol, *J. Biol. Chem.* **270**, 5882–5890.
- Segrest, J. P., Garber, D. W., Brouillette, C. G., Harvey, S. C., and Anantharamaiah, G. M. (1994) The amphipathic α helix: A multifunctional structural motif in plasma apolipoproteins. [Review], *Adv. Protein Chem.* **45**, 303–369.
- Li, W. H., Tanimura, M., Luo, C. C., Datta, S., and Chan, L. (1988) The apolipoprotein multigene family: Biosynthesis, structure,

- structure–function relationships, and evolution, *J. Lipid Res.* 29, 245–271.
36. Emmanuel, F., Steinmetz, A., Rosseneu, M., Brasseur, R., Gosselet, N., Attenot, F., Cuine, S., Seguret, S., Latta, M., Fruchart, J. C., and et al. (1994) Identification of specific amphipathic α -helical sequence of human apolipoprotein A-IV involved in lecithin: cholesterol acyltransferase activation, *J. Biol. Chem.* 269, 29883–29890.
37. Stryer, L. (1965) The interaction of a naphthalene dye with apomyoglobin and apohemoglobin. A fluorescent probe of non-polar binding sites, *J. Mol. Biol.* 13, 482–495.
38. Oram, J. F., Lawn, R. M., Garvin, M. R., and Wade, D. P. (2000) ABCA1 is the cAMP-inducible apolipoprotein receptor that mediates cholesterol secretion from macrophages, *J. Biol. Chem.* 275, 34508–34511.
39. Smith, J. D., Miyata, M., Ginsberg, M., Grigaux, C., Shmookler, E., and Plump, A. S. (1996) Cyclic AMP induces apolipoprotein E binding activity and promotes cholesterol efflux from a macrophage cell line to apolipoprotein acceptors, *J. Biol. Chem.* 271, 30647–30655.
40. Sparks, D. L., Davidson, W. S., Lund-Katz, S., and Phillips, M. C. (1993) Effect of cholesterol on the charge and structure of apolipoprotein A-I in recombinant high-density lipoprotein particles, *J. Biol. Chem.* 268, 23250–23257.
41. Weinberg, R. B., and Spector, M. S. (1985) Structural properties and lipid binding of human apolipoprotein A-IV, *J. Biol. Chem.* 260, 4914–4921.
42. Weinberg, R. B., Anderson, R. A., Cook, V. R., Emmanuel, F., Deneffe, P., Tall, A. R., and Steinmetz, A. (2002) Interfacial exclusion pressure determines the ability of apolipoprotein A-IV truncation mutants to activate cholesterol ester transfer protein, *J. Biol. Chem.* 277, 21549–21553.
43. Segall, M. L., Dhanasekaran, P., Baldwin, F., Anantharamaiah, G. M., Weisgraber, K. H., Phillips, M. C., and Lund-Katz, S. (2002) Influence of apoE domain structure and polymorphism on the kinetics of phospholipid vesicle solubilization, *J. Lipid Res.* 43, 1688–1700.
44. Natarajan, P., Forte, T. M., Chu, B., Phillips, M. C., Oram, J. F., and Bielicki, J. K. (2004) Identification of an apolipoprotein A-I structural element that mediates cellular cholesterol efflux and stabilizes ABCA1, *J. Biol. Chem.*, in press
45. Weinberg, R. B., Anderson, R. A., Cook, V. R., Emmanuel, F., Deneffe, P., Hermann, M., and Steinmetz, A. (2000) Structure and interfacial properties of chicken apolipoprotein A-IV, *J. Lipid Res.* 41, 1410–1418.
46. Rodriguez, M. D., Kalogeris, T. J., Wang, X. L., Wolf, R., and Tso, P. (1997) Rapid synthesis and secretion of intestinal apolipoprotein A-IV after gastric fat loading in rats, *Am. J. Physiol.* 272, R1170–R1177.
47. Chen, Y. H., Yang, J. T., and Martinez, H. M. (1972) Determination of the secondary structures of proteins by circular dichroism and optical rotatory dispersion, *Biochemistry* 11, 4120–4131.

BI048978M